SCIENTIFIC REPORT

A. General synthesis on the 2[nd] Stage of the project

The research team members who carried out research activities in the 2[nd] Stage of the project "Fuzzy controllers for shape memory alloys systems", no. TE 65 / 2020, project code PN-III-P1-1.1-TE-2019-1117, http://www.aut.upt.ro/~claudia.dragos/TE2019.html, consists of: Lect. Claudia-Adina BOJAN-DRAGOŞ – Director of the project, Prof. Stefan PREITL – Member, Assist. Raul-Cristian ROMAN – Member and M.Sc. Elena-Lorena HEDREA - Member.

The 2[nd] Stage of the project – The analysis, development, implementation and validation of the new control structures with adaptive fuzzy control algorithms by experiments on the laboratory equipment with SMA and on other laboratory equipment with SMA actuators and with the support of the external partners *(In Romanian – Analiza, proiectarea, implementarea și validarea noilor SRA cu regulatoarele fuzzy adaptive prin intermediul experimentelor pe echipamente de laborator în legătură cu SMA și alte echipamente de laborator cu elemente de execuție bazate pe SMA și prin intermediul partenerilor noștri externi).* – carried out during January-December 2021 has been fulfilled and is grouped in the form of the following activities:

Act 2.1 - The analysis of the actual theoretical framework with regard to the development of three adaptive fuzzy control algorithms by combination of fuzzy control and adaptive control, gain-scheduling control and sliding mode control to improve the control system performances *(In Romanian – Analiza cercetărilor actuale privind proiectarea a trei soluții de reglare fuzzy adaptivă prin combinarea reglării fuzzy cu reglarea adaptivă, reglarea gain-scheduling și reglarea în mod alunecător pentru a îmbunătății performanțele sistemelor de reglare automată).* To accomplish this activity, the analysis of the actual theoretical framework regarding the development of adaptive fuzzy control algorithms regarding controlling processes that include Shape Memory Alloys (SMA) actuators was considered. Details are presented in the study in section B.

Act 2.2 - The development of stability for the proposed control systems with the new adaptive fuzzy control algorithms using different stability methods *(In Romanian – Asigurarea stabilității SRA cu noile regulatoare fuzzy adaptive utilizând diverse metode de stabilitate).* To accomplish this activity, the analysis of stability for the control systems with adaptive fuzzy control algorithms was done using different stability methods. Details are presented in the study in section B.

Act 2.3 - The implementations, testing and validation of the new control structures with adaptive fuzzy control algorithms by simulation or by experiments on laboratory equipment with SMA and on other laboratory equipment with SMA actuators. *(In Romanian – Implementarea, testarea și validarea noilor SRA cu regulatoare fuzzy adaptive prin simulare sau prin experimente pe echipamente de laborator în legătură cu SMA si pe alte echipamente de laborator cu elemente de execuție bazate pe SMA).* To accomplish this activity, the developed adaptive fuzzy control algorithms regarding controlling processes that include Shape Memory Alloys (SMA) actuators were implemented, tested and validated on simulated laboratory equipment with SMA. Details are presented in the study in section B.

Act 2.4 - The validation of the new control structures with nonlinear controllers with the support of the external partners (Continental Automotive Timișoara, Airbus Helicopters Romania – through direct connections timely consolidated, Ontario Center of Excellence – through our Ottawa team partner) *(In Romanian – Validarea noilor SRA cu regulatoare neliniare prin intermediul partenerilor din mediul privat (Continental Automotive Timișoara, Airbus Helicopters Romania prin relații directe consolidate în timp, Ontario Center of Excellence prin intermediul partenerul nostru din Ottawa, Canada).* To accomplish this activity, the developed adaptive fuzzy control algorithms were implemented, tested, and validated on laboratory equipment with SMA from the external partners. Details are presented in the study in section B.

The main results obtained in the 2nd Stage of the project:

- cumulated impact factor according to 2020 Journal Citation Reports (JCR) released by Clarivate Analytics in 2021 = 4.672,
- **2 papers** published in Clarivate Analytics Web of Science (formerly ISI Web of Knowledge) journals with impact factors (Precup et al., 2021a; Precup et al., 2021b)
- **1 paper** accepted to be published in Clarivate Analytics Web of Science (formerly ISI Web of Knowledge)

journals with impact factors (Precup et al., 2021c),

- **2 papers** published in conference proceedings indexed in international databases (IEEE Xplore, INSPEC, Scopus, DBLP) (Bojan-Dragos et al., 2021; Hedrea et al., 2021),
- **1 paper** presented in conference proceedings to be indexed in international databases (IEEE Xplore, INSPEC, Scopus, DBLP) (Roman et al., 2021),
- **1 scientific report**.

Remarks:

- The bibliographic study related to section B is presented in section C, and the results obtained during 2021 are presented in section D.
- All published papers or accepted to be published which contains research results obtained under this project mentioned the support of UEFISCDI in the Acknowledgments section, together with the specification of the submitting code of the funding application.
- The obtained results are also mentioned in the web page of the project, http://www.aut.upt.ro/~claudia.dragos/TE2019.html, where all the information related to the development of the project will be included.

B. Development of the theoretical framework that allows the development and implementation of adaptive fuzzy control solutions

The following description is focused on the synthetic presentation of the research carried out in activities 2.1–2.4, the analysis, development, implementation, and validation of the control structures with adaptive fuzzy control algorithms with experiments performed on various laboratory equipment. The main contribution is an approach to optimally tune the parameters of type-1 and type-2 fuzzy controllers for systems, in this case Electromagnetic Actuated Clutch Systems with SMA actuators according to (Bojan-Dragos et al., 2021). The parameter vector of the fuzzy controller (of type-1 and type-2) is the vector variable of the optimization problem which is solved by a GWO algorithm that targets the minimization of a cost function expressed as the sum of squared control errors.

In the following paragraphs, details regarding the accomplishment of the ***Activity 2.1*** are presented. The nonlinearities and the variable parameters of complex processes lead to the necessity of nonlinear controllers. Such representative intelligent controllers are type-1 and type-2 fuzzy ones, which are capable to provide high control system performances because it can model and minimize the effects of certain uncertainties (Castillo et al., 2011; Castillo et al., 2016). The concept of type-2 fuzzy sets was first suggested by Lotfi A. Zadeh in 1975, shortly after the concept of type-1 fuzzy sets. It was next treated systematically in (Karnik et al., 1999; Mendel, 2001) as an extended version that can overcome the limitations of type-1 fuzzy sets and type-1 fuzzy control in handling the parametric uncertainties in the model being capable of providing an extra degree of freedom to include different uncertainties like rule uncertainties, steady-state and dynamic load-type disturbances and noise.

As shown in (Bojan-Dragos et al., 2021), an overview focused on the past, present and future of type-2 fuzzy controllers, including their theoretical and practical implications, is conducted in (Mittal et al., 2020). Some recent applications of such controllers in automotive systems are briefly discussed as follows. The tracking performance improvement and the rejection of the external disturbances of road specific to autonomous vehicles is carried out in (Taghavifar and Rakheja, 2019) using a fuzzy type-2 neural network controller with an exponential-like sliding surface. An interval type-2 fuzzy controller handles the uncertainties of driving conditions of hybrid electric autonomous vehicle in (Phan et al., 2020). A type-2 fuzzy controller is designed in (Dominik, 2016) to control the position of shape memory alloy wire actuators.

The shape change of membership functions makes the distinction between the type-1 and type-2 fuzzy systems. In type-1 ones, considering one input value, it is associated to just one membership function value in [0,1], unlike the type-2 ones, where the value of membership function form of a set of values in [0,1]. More exactly, in type-2 ones the membership functions are three-dimensional; the third dimension is the membership function value at each point on its two-dimensional domain; the name of this domain is the Footprint of Uncertainty (FOU).

In many applications, the desired performance indices (rise time, settling time, overshoot etc.) and the integral- or sum-type cost functions in properly defining optimization problems can be guarantee by the design and tuning of fuzzy control systems as shown in (Guerra et al., 2015; Precup et al., 2015). However, setting the optimization problems representative to the optimal tuning of fuzzy controllers is not simple especially in case of type-2 fuzzy ones because of the expressions of the cost functions and the risk to get trapped in local minima. Nature-inspired optimization algorithms as the popular swarm intelligence algorithms can be useful to minimize these cost functions as they exhibit reduced computational cost, transparency, and cost-effective design and implementation. Such algorithms include. Representative overviews on swarm intelligence algorithms in fuzzy control including type-2 fuzzy control are given in (Castillo et al., 2012; Castillo and Melin, 2014; Precup and David, 2019).

The contribution of the team research members is important regarding the similar solutions studied in literature in the field since many current fuzzy controllers are of Mamdani type, while this paper employs Takagi-Sugeno fuzzy controllers. In addition, it is difficult to control this kind of nonlinear process with SMA actuators and fuzzy control proves to be an initially relatively simple nonlinear control to cope with it. The type-2 Takagi-Sugeno controllers considered here use type-2 membership functions only for their input variables. The results are validated using simulation results and confirm the efficiency of control system with optimal Takagi-Sugeno type-2 fuzzy controllers.

The Grey Wolf Optimizer (GWO) algorithm (Mirjalili et al., 2014) is a recent and successful swarm intelligence algorithm developed by mimicking grey wolf social hierarchy and hunting habits. It offers very good results including applications to fuzzy control reported in (Noshadi et al., 2016; Precup et al., 2016; Precup et al., 2017a).

The reduction of the sum of squared control error is ensured by the following optimization problems

$$\boldsymbol{\rho}^{(j)*} = \arg \min_{\boldsymbol{\rho}^{(j)} \in D_\rho} J(\boldsymbol{\rho}^{(j)}) = \frac{1}{M}\sum_{k=1}^{N}[y_k^*(\boldsymbol{\rho}^{(j)}) - y_k(\boldsymbol{\rho}^{(j)})]^2 = \frac{1}{M}\sum_{k=1}^{N} e_k^2(\boldsymbol{\rho}^{(j)}), \quad (1)$$

where j denotes the controller type, $j \in \{\text{PI, TS-T1-FC, TS-T2-FC}\}$, the abbreviation TS-T1-FC is used for the adaptive Takagi-Sugeno type-1 fuzzy controller, the abbreviation TS-T2-FC is used for the adaptive Takagi-Sugeno type-2 fuzzy controller, $e_k(\boldsymbol{\rho}^{(j)}) = y_k^*(\boldsymbol{\rho}^{(j)}) - y_k(\boldsymbol{\rho}^{(j)})$ is the control error at k^{th} sampling interval, $y_k^*(\boldsymbol{\rho}^{(j)})$ is the reference input (the set-point), $y_k(\boldsymbol{\rho}^{(j)})$ is the controlled output, $\boldsymbol{\rho}^{(j)}$ is the controller parameter vector, D_ρ is the feasible domain of $\boldsymbol{\rho}^{(j)}$, and $\boldsymbol{\rho}^{(j)*}$ is the optimal controller parameter vector. The cost function $J(\boldsymbol{\rho}^{(j)})$ is a performance index that assesses the performance of the control system, and M in (1) s the length of the time horizon.

The initialization of the agents (i.e., wolves) is the first step GWO algorithms as pointed before in (Mirjalili et al., 2014) comprising the pack. Each agent of a total number of used N agents (i.e., grey wolves) will be modelled by its position vector $\mathbf{X}_i(\mu)$

$$\mathbf{X}_i(\mu) = [x_i^1(\mu) \quad \dots \quad x_i^f(\mu) \quad \dots \quad x_i^q(\mu)]^T, \; i = 1 \dots N, \quad (2)$$

where $x_i^f(\mu)$ is the position of i^{th} agent in f^{th} dimension, $f = 1 \dots q$, μ is the index of the current iteration, $\mu = 1 \dots \mu_{\max}$, and $\mu_{\max}$ is the maximum number of iterations. Additional details on the GWO algorithm that is implemented in this paper and the associated vector operations are given in (Precup et al., 2016; Precup et al., 2017a; Precup et al., 2017b).

The GWO algorithm is mapped onto the optimization problems defined in (1) in terms of the following relationships:

$$\boldsymbol{\rho}^{(j)} = \mathbf{X}_i(\mu), \; i = 1 \dots N, \quad (3)$$

$$\boldsymbol{\rho}^{(j)*} = \arg \min_{i=1 \dots N} J(\mathbf{X}_i(\mu_{\max})), \quad (4)$$

and the numbers of tuning parameters of the three controllers, with $j \in \{\text{PI, TS-T1-FC, TS-T2-FC}\}$, are q.

The presentation of the adaptive fuzzy controller structures and their design approach starts with outlining the theoretical support of TS-T1-FC. The design of the TS-T1-FC is based on the design of continuous-time PI controllers, where good recommendations are given in (Åström and Hägglund, 1995). The transfer function of a PI controller is C_{PI}

$$C_{PI}(s) = k_C(1+T_c s)/(T_c s), \quad (5)$$

where k_C is the controller gain and T_c is its integral time constant.

The PI controller is discretized using Tustin's method with the sampling period T_s to obtain the equations of the discrete-time PI controller in its incremental form widely used in quasi-continuous digital control (Precup and David, 2019)

$$\Delta u_k = \gamma(\eta K_P \Delta e_k + K_I e_k),$$
$$K_P = k_C(1 - T_s/(2T_c)),\ K_I = k_C T_s / T_C, \quad (6)$$

where: e_k – the control error, Δe_k – the increment of control error, Δu_k – the increment of control signal, K_P and K_I – the parameters of the digital PI controller, and the additional parameters γ and η allow the improvement of the input-output map of the fuzzy controller in order to modify and adjust the control system performance.

The first equation in (6) indicates that the parameters γ and η are not needed and their presence increases artificially the number of tuning parameters of TS-T1-FC. They can be dropped out and included in K_P and K_I, and thus reduce the number of tuning parameters with two and the search space as well. However, these two parameters are kept in the design to highlight that the fuzzy controller design starts here with the design of the linear PI controller, and the knowledge from that is next transferred to the fuzzy controller structure and design. This motivation is also used as far as TS-T2-FC is concerned. In addition, the input variables of both TS-T1-FC and TS-T2-FC are also scheduling variables.

In this regard, the rule base of the TS-T1-FC with the linear PI controllers in its consequents is

$$\text{Rule 1: IF } e_k \text{ IS N AND } \Delta e_k \text{ IS P THEN } \Delta u_k = \gamma^1[\eta^1 K_P \Delta e_k + K_I e_k],$$
$$\ldots \quad (7)$$
$$\text{Rule n: IF } e_k \text{ IS P AND } \Delta e_k \text{ IS N THEN } \Delta u_k = \gamma^n[\eta^n K_P \Delta e_k + K_I e_k].$$

Linguistic terms (LTs) with uniform distribution membership functions, whose optimal parameters will be obtained in the next section according to the GWO algorithm, are employed. The inference engine uses the MIN and MAX operators in relation with the rule base in (7), and the weighted average method for defuzzification is included in TS-T1-FC structure.

Fig. 1 illustrates the block diagram of a adaptive TS-2-FC structure. It includes five sub-systems: fuzzifier, rule base, inference engine, type-reducer and defuzzifier. The inputs are the control error and its increment, and a single output is used, in TS-2-FC considered in paper and built around a linear PI controller, namely the increment of control signal.

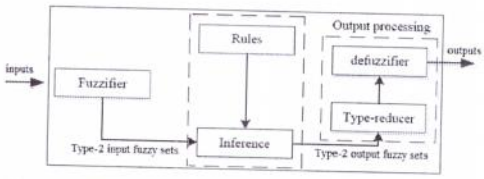

Fig. 1. Structure of type-2 fuzzy controller (Phan et al., 2020).

The rules remain the same as in TS-T1-FC, but the antecedents and the consequents are described by type 2 fuzzy sets. The rest of sub-systems operate in TS-T2-FC in the same manner as in TS-T1-FC.

But the main difference between TS-T1-FC and TS-T2-FC is that the second one employs type 2 fuzzy sets, and this it includes an extra process which is known as the essential type-reducer sub-system. Karnik and Mendel (1998) designed a popular type-reducer, which calculates the centroids of type 2 sets and of the type-reduced set. While using the usual centroid type-reduced the firing output set is generated from by each fuzzy rule.

The GWO-based tuning approach that ensures the optimal tuning of TS-T1-FC and TS-T2-FC consists of three steps:

Step A. A linear tuning method is applied to initially obtain the parameters of the linear PI controllers, then T_s is fixated and the discrete-time PI controllers in (6) are achieved.

Step B. The dynamic regime involved in the evaluation of the cost function in (1) is defined. This includes the setting of the time horizon which includes all transients of the fuzzy control system until the cost function will obtain the value of steady-state. All constraints imposed to the elements of $\boldsymbol{\rho}^{(j)}$ are included in the feasible domain D_{ρ}.

Step C. The GWO algorithms are used to calculate the optimal parameter vector $\boldsymbol{\rho}^{(j)*}$.

The tuning approach detailed earlier was applied to the optimal tuning of first a linear PI controller ad next two Takagi-Sugeno PI-fuzzy controllers, represented by TS-T1-FC and TS-2FC. All these controllers are dedicated to the position control of the electromagnetic actuated clutch system with SMA actuators described in the next.

The process considered in this paper is an electromagnetic actuated clutch system with SMA actuators as part of electric drive clutches. Its structure is given in Fig. 2. The controllers are designed and tuned considering the mass position as controlled output.

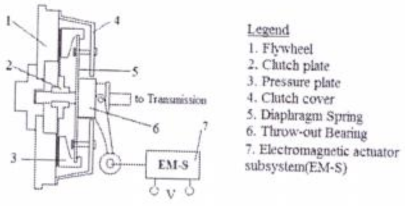

Fig. 2. Electromagnetic actuated clutch system (Di Cairano et al., 2017).

Simplified nonlinear models can be accepted by neglecting the nonlinearities of the plant which are analysed in complete form and are included in the equation of the motion; the mechanical subsystem has the following dynamics

$$m\ddot{x} = F - c\dot{x} - kx, \tag{8}$$

and it is actuated by an electromagnetic subsystem with nonlinear characteristics. Its dynamic behaviour is characterized by (Di Cairano et al., 2007)

$$\begin{aligned} &\dot{\lambda} = V - Ri, \quad \lambda = 2k_a i/(k_b + d - x), \\ &F = k_a i^2/(k_b + d - x)^2 = \lambda^2/(4k_a). \end{aligned} \tag{9}$$

The process parameters that appear in (8) and (9) have the numerical values adopted starting with (Di Cairano et al., 2007) and are synthesized in Table 1.

Table 1. Numerical values of process parameters

Symbols	Parameters	Numerical Values	Measurement Units
M	Mass	1	Kg
X	Mass positions	0÷0.004	M
D	The difference between contact position	0.004	M
k	Spring's stiffness	37500	N/m
C	Damper's coefficient	700	N·s/m
k_b	Constant	0.375	
k_a	Constant	0.5	
F	External force	0÷150	N
Λ	Magnetic flux		V·s
I	Current	0 ÷ 10	A
V	Control signal	0÷12	V
R	Resistance	1.2	Ω

In the following paragraphs, details regarding the accomplishment of the ***Activity 2.2*** are presented. The stability analysis of the proposed CS is presented as follows. This stability analysis is also carried out in (Bojan-Dragos et al., 2019; Hedrea et al., 2019; Precup et al., 1999; Precup et al., 2020). Similar fuzzy controllers are used in (Bojan-Dragos et al., 2019; Hedrea et al., 2019) but the nonlinear process controlled is different. For performing the stability analysis, the dynamics of the fuzzy controller (FC) is transferred to the process, and this leads to the extended controlled process (EP), illustrated in Fig. 3 (Precup and Preitl, 1997). For the sake of simplicity the stability analysis is presented below in an unified manner for both control structures, where $\mathbf{w}_k = [w_k \quad \Delta w_k]^T$ with w_k the reference input, $\Delta w_k = w_k - w_{k-1}$ the increment of reference input, $\mathbf{e}_k = [e_k \quad \Delta e_k]^T$, with: e_k the control error, Δe_k the increment of control error, $\mathbf{y}_k = [y_k \quad \Delta y_k]^T$, with: y_k the controlled output, $\Delta y_k = y_k - y_{k-1}$ the increment of controlled output, $\mathbf{u}_k = [\Delta u_k \quad \Delta u_{fk}]^T$, where u_{fk} represents the fictitious control signal, Δu_{fk} stands for the fictitious increment of control signal, $\Delta u_{fk} = u_{fk} - u_{fk-1}$ (Bojan-Dragos et al., 2019; Hedrea et al., 2019; Precup and Preitl, 1997; Precup and Preitl, 2003).

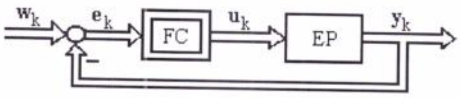

Fig. 3. Modified structure of fuzzy CS.

The FC block is characterized by the nonlinear input-output static map **F**

$$\mathbf{F}: R^2 \to R^2, \mathbf{F}(\mathbf{e}_k) = [f(\mathbf{e}_k) \quad 0]^T, \tag{10}$$

where $f\,(f: R^2 \to R)$ is the input-output static map of the nonlinear block without dynamics inserted for steady-state and dynamic CS performance improvement.

The state-space mathematical models are next expressed as:

$$\begin{aligned} \mathbf{x}_{k+1} &= \mathbf{A}\ \mathbf{x}_k + \mathbf{B}\mathbf{u}_k, \\ \mathbf{y}_k &= \mathbf{C}\mathbf{x}_k, \end{aligned} \tag{11}$$

by inserting additional state variables, which result in the augmented state vectors $\mathbf{x}_k = [\mathbf{x}_k \quad x_{uk} \quad x_{yk}]^T$, due to the presence of the additional linear dynamics transferred from the fuzzy PI controller structures, (Bojan-Dragos et al., 2019; Hedrea et al., 2019; Precup and Preitl, 1997; Precup and Preitl, 2003).

Therefore, the resulting state-space matrices are

$$\begin{aligned} &\mathbf{A} = \begin{bmatrix} \mathbf{A} & \mathbf{b} & \mathbf{0} \\ \mathbf{0}^T & 1 & 0 \\ \mathbf{c}^T & 0 & 0 \end{bmatrix}, \mathbf{B} = \begin{bmatrix} \mathbf{b} & \mathbf{1} \\ 1 & 1 \\ 0 & 1 \end{bmatrix}, \mathbf{C} = \begin{bmatrix} \mathbf{c}^T & 0 & 0 \\ \mathbf{c}^T & 0 & -1 \end{bmatrix}, \\ &\mathbf{A} \in \Re^{nxn}, \mathbf{B} \in \Re^{nx2}, \mathbf{C} \in \Re^{2xn}, \end{aligned} \tag{12}$$

where n is the order of the mathematical models.

The structure presented in Fig. 4 is used in the stability analysis of the nonlinear CS, where the NL block represents a static nonlinearity due to the nonlinear part without dynamics of the FC block.

The connections between the variables of the CS structures in Figs. 3 and 4 are

$$\mathbf{v}_k = -\mathbf{u}_k = -\mathbf{F}(\mathbf{e}_k), \mathbf{y}_k = -\mathbf{e}_k, \tag{13}$$

where the second component of **F** is always zero in order to neglect the effect of fictitious control signal.

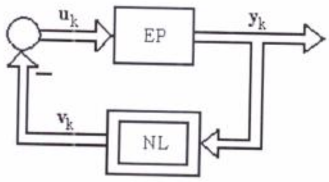

Fig. 4. Structure of nonlinear control system involved in stability analysis.

By taking into account the relation (13), the second equations in (11) become:

$$\mathbf{e}_k = -\mathbf{C}\mathbf{u}_k, \mathbf{x}_k = \mathbf{C}^b\mathbf{e}_k, \tag{14}$$

where the matrix $\mathbf{C}^b$, ($\mathbf{C}^b \in \Re^{nx2}$), can be computed relatively easily as function of **C**.

The stability analysis theorem is (Precup and Preitl, 1997; Precup and Preitl, 2003):

Theorem 1. The nonlinear system whose structure is given in Fig. 4 and whose mathematical model is presented (11) is globally asymptotically stable if the conditions I and II are fulfilled by the matrices **P**, **L** and **V**:

I.

$$\begin{aligned} (\mathbf{A})^T\mathbf{P}\cdot\mathbf{A} &= -\mathbf{L}\,\mathbf{L}^T, \\ \mathbf{C}-(\mathbf{B})^T\mathbf{P}\cdot\mathbf{A} &= \mathbf{V}^T\mathbf{L}^T, \\ -(\mathbf{B})^T\mathbf{P}\cdot\mathbf{B} &= \mathbf{V}^T\mathbf{V}. \end{aligned} \tag{15}$$

II. By introducing the matrices **M** ($\mathbf{M}\in\Re^{2x2}$), **N** ($\mathbf{N}\in\Re^{2x2}$) and **R** ($\mathbf{R}\in\Re^{2x2}$) defined as follows:

$$\begin{aligned} &\mathbf{M} = (\mathbf{C}^b)^T(\mathbf{L}\,\mathbf{L}^T - \mathbf{P})\mathbf{C}^b, \quad \mathbf{R} = \mathbf{V}^T\mathbf{V}, \\ &\mathbf{N} = (\mathbf{C}^b)^T[\mathbf{L}\,\mathbf{V} - (\mathbf{A})^T\mathbf{P}\,\mathbf{B}^a - 2(\mathbf{C})^T, \end{aligned} \tag{16}$$

the next inequality holds for any value of control error e_k:

$$f(\mathbf{e}_k)\mathbf{n}^T\mathbf{e}_k + (\mathbf{e}_k)^T\mathbf{M}\,\mathbf{e}_k \geq 0, \tag{17}$$

where the vector $\mathbf{e}_k$ is defined in (13) and **n** represents the first column of **N**.

Proof. The first condition (I) represents the first equation from the Kalman-Szegö lemma; therefore, it is fulfilled (Landau, 1979).

In order to fulfil the second condition (II), the Popov inequality (17), which ensures the global asymptotic stability of the nonlinear CS for any positive constant β_0, is expressed:

$$S(k_1) = \sum_{k=0}^{k_1}(\mathbf{v}_k)^T\mathbf{y}_k \geq -\beta_0^2 \quad \forall k_1 \in N^*. \tag{18}$$

Considering (13), the Popov sum $S(k_1)$ becomes:

$$S(k_1) = -\sum_{k=0}^{k_1} (\mathbf{u}_k)^T \mathbf{y}_k \quad \forall k_1 \in N^*. \tag{19}$$

By substituting in (19) the expression of $\mathbf{x}_{k+1}$ and $\mathbf{y}_k$ from (11), followed by adding and subtracting the term $(\mathbf{x}_{k+1})^T \mathbf{P} \cdot \mathbf{x}_{k+1}$ and using the properties of matrix transposition the Popov sum $S(k_1)$ becomes:

$$\begin{aligned} S(k_1) = -\sum_{k=0}^{k_1} \{ & -(\mathbf{x}_k)^T (\mathbf{A})^T \mathbf{P} \cdot \mathbf{A}\mathbf{x}_k - (\mathbf{x}_k)^T [(\mathbf{A})^T (\mathbf{P} + +\mathbf{P}^T)\mathbf{B} + \\ & (\mathbf{C})^T]\mathbf{u}_k - (\mathbf{u}_k)^T (\mathbf{B})^T \mathbf{P} \cdot \mathbf{B} \cdot \mathbf{u}_k + (\mathbf{x}_{k+1})^T \mathbf{P} \cdot \mathbf{x}_{k+1}]\} \quad \forall k_1 \in N^*. \end{aligned} \tag{20}$$

By replacing the expressions of $(\mathbf{A})^T \mathbf{P} \cdot \mathbf{A}$, $(\mathbf{A})^T \mathbf{P}^T \cdot \mathbf{B}$ and $(\mathbf{B})^T \mathbf{P} \cdot \mathbf{B}$ from the condition (I) and by expressing $\mathbf{x}_k$ from (14) and using the condition (II), another form of the Popov sum $S(k_1)$ is obtained:

$$S(k_1) = -\sum_{k=0}^{k_1} (\mathbf{x}_{k+1})^T \mathbf{P} \cdot \mathbf{x}_{k+1} + \sum_{k=0}^{k_1} [(\mathbf{e}_k)^T \mathbf{M} \cdot \mathbf{e}_k + (\mathbf{e}_k)^T \mathbf{N} \cdot \mathbf{u}_k + (\mathbf{u}_k)^T \mathbf{R} \cdot \mathbf{u}_k] \quad \forall k_1 \in N^*. \tag{21}$$

Using the expression of $\mathbf{u}_k$ in (13), (21) becomes:

$$S(k_1) = -\sum_{k=0}^{k_1} (\mathbf{x}_{k+1})^T \mathbf{P} \cdot \mathbf{x}_{k+1} + \sum_{k=0}^{k_1} [(\mathbf{e}_k)^T \mathbf{M} \cdot \mathbf{e}_k + (\mathbf{e}_k)^T \mathbf{N} \cdot \mathbf{F}(\mathbf{e}_k) + \mathbf{F}^T(\mathbf{e}_k) \mathbf{R} \cdot \mathbf{F}(\mathbf{e}_k)] \quad \forall k_1 \in N^*. \tag{22}$$

Finally, the expression of the sum $S(k_1)$ is obtained by using $\mathbf{F}$ from (10) and the positive element r_{11} of matrix $\mathbf{R}$:

$$S(k_1) = -\sum_{k=0}^{k_1} [(\mathbf{x}_{k+1})^T \mathbf{P} \cdot \mathbf{x}_{k+1} + r_{11} f^2(\mathbf{e}_k)] + \sum_{k=0}^{k_1} [(\mathbf{e}_k)^T \mathbf{M} \cdot \mathbf{e}_k + f(\mathbf{e}_k) \mathbf{n}^T \cdot \mathbf{e}_k] \quad \forall k_1 \in N^*. \tag{23}$$

Both sums in (23) are positive and therefore the sum $S(k_1)$ is also positive, which means that the condition (II) guarantees the fulfilment of the Popov inequality (18). In conclusion, the fuzzy CS globally asymptotically stable, therefore Theorem 1 is proved.

For $n > 2$, only the matrix $\mathbf{P}$ from the first condition (I) is significant for the fuzzy CS stability analysis because the matrices $\mathbf{M}$, $\mathbf{N}$ and $\mathbf{R}$ from the second condition (II) can be expressed as functions of $\mathbf{P}$.

$$\begin{aligned} & \mathbf{M} = -(\mathbf{C}^b)^T (\mathbf{A})^T \mathbf{P} \cdot \mathbf{A}\mathbf{C}^b, \ \mathbf{R} = -(\mathbf{B})^T \mathbf{P} \cdot \mathbf{B}, \\ & \mathbf{N} = -(\mathbf{C}^b)^T [(\mathbf{A})^T (\mathbf{P} + \mathbf{P}^T)\mathbf{B} + (\mathbf{C})^T]. \end{aligned} \tag{24}$$

The approach presented in this sub-section is different to the stability analysis approach presented in Section II, which is based on LMIs. This might lead to the conclusion that the stable design of the controllers in this paper is non-homogenous. However, both approaches have the same feature, namely they depend on the process model. The reduction of process parametric sensitivity can be treated to alleviate this shortcoming or model–free control can be employed, but the latter is difficult to be related to stability because of the lack of parametric models in controller tuning. A general stable design approach to state-feedback control is given in (Pozna and Precup, 2018), and a stable design approach to fuzzy control systems is given (Precup et al., 2014); both approaches avoid the LMIs, however they depend on the process models.

In the following paragraphs, details regarding the accomplishment of the ***Activity 2.3*** are presented. The sampling period has been set in step A to $T_s = 0.01$ s in order to implement quasi-continuous digital controllers. The feasible domains of $\boldsymbol{\rho}^{(j)}$ in terms of the three optimization problems used as search spaces were set appropriately.

The dimensions of the feasible domains (and also search spaces) are q=2 for the PI controller, q=12 for TS-T1-FC and q=7 for TS-T2-FC. The dynamic regime in step B is characterized by zero initial conditions and the 2 mm step modification of the reference input on a time horizon of 1.2 s.

The values of the parameters of the GWO algorithms that solves in step C the optimization problems in (1) were set as follows in order to ensure an acceptable trade-off to convergence speed and accuracy: the number of the agents N = 500 and the maximum number of iterations $\mu_{\max} = 20$.

The particular expression of the parameter vector of the PI controller given in (6) is

$$\boldsymbol{\rho}^{(1)} = [k_c \quad T_c]^T, \tag{25}$$

where T stands for matrix transposition, the particular expressions of the parameter vector of TS-T1-FC is

$$\begin{aligned}\boldsymbol{\rho}^{(2)} = [&B_e \quad B_{\Delta e} \quad \gamma^1 \quad \eta^1 \quad \gamma^2 \quad \eta^2 \\ &\gamma^3 \quad \eta^3 \quad \gamma^4 \quad \eta^4 \quad \gamma^5 \quad \eta^5]^T,\end{aligned} \tag{26}$$

where B_e and $B_{\Delta e}$ are the parameters of the membership functions of the input LTs, and the parameters γ^i, $i = 1...5$, and η^i, $i = 1...5$, introduce extra nonlinearities to adjust the performance of the control systems. The particular expressions of the parameter vector of TS-T2-FC described above is

$$\boldsymbol{\rho}^{(3)} = [L_l \quad L_{sf1} \quad L_{sf2} \quad L_{sf3} \quad L_{sf4} \quad L_{sf5} \quad L_{sf6}]^T, \tag{27}$$

where L_l is the lower membership function lag value and L_{scfi}, i = 1...6, is the lower membership function scaling factor for the membership function of both input variables.

The application of a GWO algorithm leads to the following optimal tuning parameter vectors of the PI controller which ensure the system stability because the stability conditions are checked to validate the next solution candidate:

$$\boldsymbol{\rho}^{(1)*} = [74.7688 \quad 0.0898]^T. \tag{28}$$

The fuzzification sub-system in TS-T1-FC makes use of the LTs attributed to the input and also scheduling variables e_k and Δe_k, defined in the following two cases, 11 and 12.

Case 11. Three LTs with trapezoidal and triangular membership functions for both input variables are used. The following nine rules with the parameters $K_P = 6.34$ and $K_I = 0.38$ of the PI controllers placed in the rule consequents leads to the complete rule base of TS-T1-FC:

$$\begin{aligned}
&\text{Rule 1: IF } e_k \text{ IS N AND } \Delta e_k \text{ IS N THEN } \Delta u_k = \gamma^5[\eta^5 K_P \Delta e_k + K_I e_k],\\
&\text{Rule 2: IF } e_k \text{ IS N AND } \Delta e_k \text{ IS ZE THEN } \Delta u_k = \gamma^4[\eta^4 K_P \Delta e_k + K_I e_k],\\
&\text{Rule 3: IF } e_k \text{ IS N AND } \Delta e_k \text{ IS P THEN } \Delta u_k = \gamma^3[\eta^3 K_P \Delta e_k + K_I e_k],\\
&\text{Rule 4: IF } e_k \text{ IS ZE AND } \Delta e_k \text{ IS N THEN } \Delta u_k = \gamma^2[\eta^2 K_P \Delta e_k + K_I e_k],\\
&\text{Rule 5: IF } e_k \text{ IS ZE AND } \Delta e_k \text{ IS ZE THEN } \Delta u_k = \gamma^1[\eta^1 K_P \Delta e_k + K_I e_k],\\
&\text{Rule 6: IF } e_k \text{ IS ZE AND } \Delta e_k \text{ IS P THEN } \Delta u_k = \gamma^2[\eta^2 K_P \Delta e_k + K_I e_k],\\
&\text{Rule 7: IF } e_k \text{ IS P AND } \Delta e_k \text{ IS N THEN } \Delta u_k = \gamma^3[\eta^3 K_P \Delta e_k + K_I e_k],\\
&\text{Rule 8: IF } e_k \text{ IS P AND } \Delta e_k \text{ IS N THEN } \Delta u_k = \gamma^4[\eta^4 K_P \Delta e_k + K_I e_k],\\
&\text{Rule 9: IF } e_k \text{ IS P AND } \Delta e_k \text{ IS P THEN } \Delta u_k = \gamma^5[\eta^5 K_P \Delta e_k + K_I ee_k].
\end{aligned} \tag{29}$$

The GWO algorithm applied in the terms given above conducts to the following optimal tuning parameter vector of TS-T1-FC which ensures the system stability:

$$\boldsymbol{\rho}^{(2)*} = [13.8252\ 19.6579\ 5.7156\ 0.2461\ 5.9587\ 0.1515\ 5.736\ 0.087\ 3.4285\ 0.2577\ 3.6969\ 0.0558]^T. \tag{30}$$

Case 12. Three LTs with a spline-based Z-shaped membership function, a Gaussian membership function and a spline-based S-shaped membership function for both input variables are used. The same complete rule base given in (14) was used. The GWO-based solving of (3) leads to the following optimal tuning parameter vector of TS-T1-FC which ensures the system stability:

$$\boldsymbol{\rho}^{(2)*} = [16.6814\ 12.9926\ 1.4641\ 0.5128\ 1.1202\ 0.0883\ 0.9555\ 0.0894\ 0.8646\ 0.2625\ 1.0427\ 0.1069]^T. \quad (31)$$

Two cases were also considered for the input variables in the fuzzification sub-system of TS-T2-FC, 21 and 22, with the results described as follows.

Case 21. The membership function distribution for particular inputs of the TS-T2-FC is trapezoidal and triangular (Fig. 5), with the value of FOU optimally tuned by a GWO algorithm. The enhanced Karnik-Mendel method was implemented in the type-reducer sub-system.

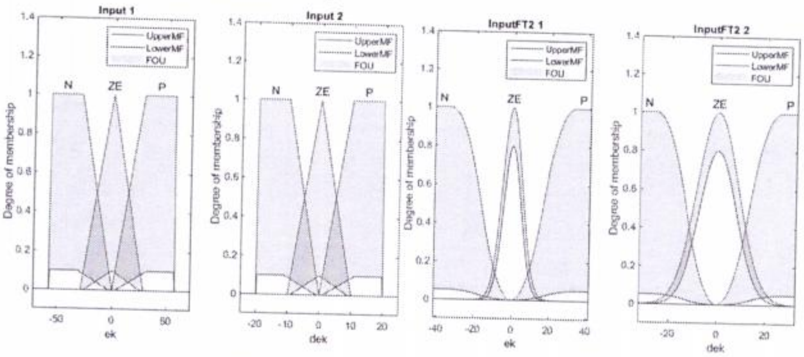

Fig. 5. Input membership functions in cases 21 and 22.

The GWO algorithm conducts to the following optimal tuning parameter vector of TS-T2-FC which ensures the system stability:

$$\boldsymbol{\rho}^{(3)*} = [0.1\quad 0.1\quad 0.1\quad 0.1\quad 0.1\quad 0.1\quad 0.1]^T. \quad (32)$$

Case 22. A spline-based Z-shaped membership function, a Gaussian membership function and a spline-based S-shaped membership function (illustrated in Fig. 3) were used, with the value of FOU obtained on the basis of a GWO algorithm. The GWO algorithm leads to the following optimal tuning parameter vector of TS-T2-FC which ensures the system stability:

$$\boldsymbol{\rho}^{(3)*} = [0.0251\ 0.051\ 0.8\ 0.051\ 0.051\ 0.8\ 0.051]^T. \quad (33)$$

To highlight the difference between the control systems with the developed adaptive fuzzy control algorithms some simulation scenarios were done. Therefore, the proposed adaptive fuzzy control algorithms were tested and validated on simulated laboratory equipment with SMA actuators. The simulation scenarios are characterized by the application of a set of step-type modifications of the reference input.

The simulation results illustrated in Fig. 6 give the response of the control system with TS-T1-FC obtained in the cases 11 and 12 illustrating the measured position in time. The simulation results illustrated in Fig. 7 give the response of the control system with TS-T2-FC obtained in the cases 21 and 22, also illustrating the measured position in time. The simulation results presented in Fig. 8 show the response of the control system with TS-T1-FC obtained in the cases 11 and with TS-T2-FC obtained in the case 21 illustrating the measured position in time, which is similar to the other figures considered here. Finally, the simulation results presented in Fig. 9 show the response of the control system with TS-T1-FC obtained in the cases 12 and with TS-T2-FC obtained in the case 22, illustrating the measured position in time.

The measured value of the cost functions are $J(\boldsymbol{\rho}^{(\text{TS-T1-FC})}) = 0.1055$ in the case 11, $J(\boldsymbol{\rho}^{(\text{TS-T2-FC})}) = 0.0888$ in the case 21, $J(\boldsymbol{\rho}^{(\text{TS-T1-FC})}) = 0.0875$ in the case 21 and $J(\boldsymbol{\rho}^{(\text{TS-T2-FC})}) = 0.0853$ in the case 22.

The presented results show very good control system expressed in terms of small cost function values. Therefore, the proposed adaptive fuzzy controllers are validated by simulation results. The good performances are obtained by the adaptive fuzzy control system with TS-T2-FC.

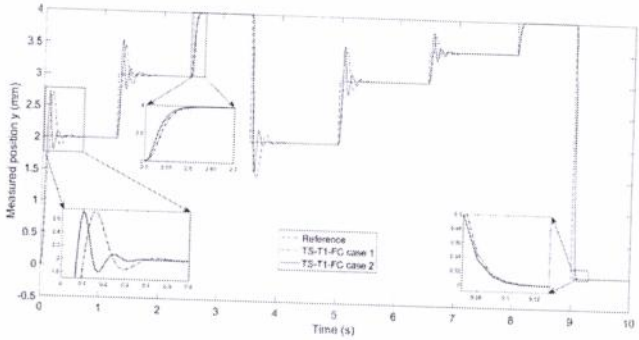

Fig. 6. Position versus time obtained in the cases 11 and 12 concerning the control system with TS-T1-FC.

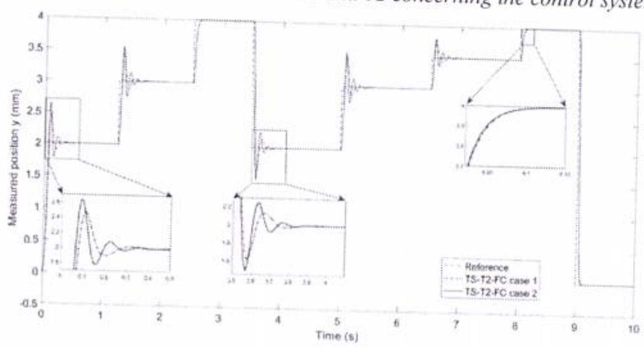

Fig. 7. Position versus time obtained in the cases 21 and 22 concerning the control system with TS-T2-FC.

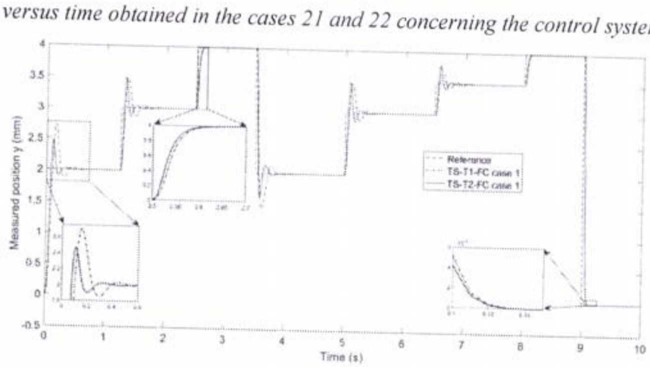

Fig. 8. Position versus time obtained in the case 11 concerning the control system with TS-T1-FC and the case 21 concerning the control system with TS-T2-FC.

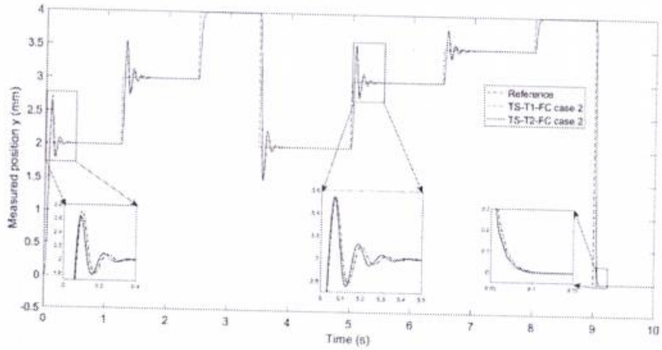

Fig. 9. Position versus time obtained in *the case 12 concerning the control system with TS-T1-FC and the case 22 concerning the control system with TS-T2-FC.*

In the following paragraphs, details regarding the accomplishment of the ***Activity 2.4*** are presented. The developed adaptive fuzzy control algorithms presented in (Bojan-Dragos et al., 2021) were tested and validated on electromagnetic actuated clutch systems with SMA actuators laboratory equipment from the Gheorghe Asachi" Technical University of Iasi, Romania through our external partner Prof. Corneliu Lazar and his team.

The evolving Takagi-Sugeno-Kang fuzzy models that characterize the position of shape memory alloy (SMA) wire actuators obtained in (Precup et al., 2021c) were also tested against the experimental data from the laboratory equipment from the Gheorghe Asachi" Technical University of Iasi, Romania through our external partner Prof. Corneliu Lazar and his team and from the laboratory equipment from the University of Ljubljana, Slovenia, in cooperation with Prof. Igor Škrjanc and Prof. Sašo Blažič and their teams. The experimental results were analyzed and compared and it turned out that the proposed fuzzy models were consistent with training and validation data.

All control solutions proposed in (Precup et al., 2021a; Precup et al., 2021b) and (Roman et al., 2021) which include sliding mode and fuzzy control and slime mould algorithm-based tuning of cost-effective fuzzy controllers, developed for servo processes with SMA actuators were also tested and validated on laboratory equipment from Ontario Centers of Excellence – through our Ottawa team partner and his team.

The iterative feedback tuning algorithm proposed in (Roman et al., 2021) for the controlling of a tower crane systems with SMA actuators were also tested and validated on laboratory equipment from Bremen University, Germany, through our team partner Prof. Axel Gräser and his team.

The tensor product-based model transformation technique proposed in (Hedrea et al., 2021) was validated by experiments on a servo system laboratory equipments from University of Debrecen, Hungary, in cooperation with Prof. Péter Korondi and from Szechenyi Istvan University, Gyor, Hungary, in cooperation with Prof. Péter Baranyi and his team. The obtained experimental results show that the TP model derived for this system ensures good performance in terms of small relative modeling errors.

C. References

Åström, K.-J. and Hägglund, T. (1995). PID controllers theory: design and tuning. Instrument Society of America, Research Triangle Park.

Bojan-Dragos, C.-A., Hedrea E.-L., Precup R.-E., Szedlak-Stinean A.-I., and Roman R.-C. (2019). MIMO fuzzy control solutions for the level control of vertical two tank systems. in Proc. 16th Int. Conf. Control, Autom. Robotics, Prague, Czech Republic, 1, 810–817.

Castillo, O., Amador-Angulo, L., Castro, J.R., and García Valdez, M. (2016). A comparative study of type-1 fuzzy logic systems, interval type-2 fuzzy logic systems and generalized type-2 fuzzy logic systems in control problems. Information Sciences, 354, 257-274.

Castillo, O., Martinez-Marroquin, R., Melin, Valdez, P.F., and Soria, J. (2012). Comparative study of bio-inspired algorithms applied to the optimization of type-1 and type-2 fuzzy controllers for an autonomous mobile robot. Information Sciences, 192, 19-38.

Castillo, O. and Melin, P. (2014). A review on interval type-2 fuzzy logic applications in intelligent control. Information Sciences, 279, 615-631.

Castillo, O., Melin, P., Garza, A.A., Montiel, O., and Sepúlveda, R. (2011). Optimization of interval type-2 fuzzy logic controllers using evolutionary algorithms. Soft Computing, 15 (6), 1145-1160.

Di Cairano, S., Bemporad, A., Kolmanovsky, I.V., and Hrovat, D. (2007). Model predictive control of magnetically actuated mass spring dampers for automotive applications. International Journal of Control, 80 (1), 1701-1716.

Dominik, I. (2016). Type-2 fuzzy logic controller for position control of shape memory alloy wire actuator. Journal of Intelligent Material Systems and Structures, 27 (14), 1917-1926.

Hedrea, E.-L., Precup, R.-E., Bojan-Dragos, C.-A. and Hedrea, C., (2019) Cascade control solutions for maglev systems, in Proc. 23nd ICSTCC, Sinaia, Romania, 20–26.

Guerra, T.-M., Sala, A., and Tanaka, K. (2015). Fuzzy control turns 50: 10 years later. Fuzzy Sets and Systems, 281, 168-182.

Karnik, N.N. and Mendel, J.M. (1998). Introduction to type-2 fuzzy logic systems. Proceedings of 1998 IEEE International Conference on Fuzzy Systems, Anchorage, AK, USA, 915-920.

Karnik, N.N., Mendel, J.M., and Liang, Q. (1999). Type-2 fuzzy logic systems. IEEE Transactions on Fuzzy Systems, 7 (6), 643-658.

Landau, I. D. (1979). Adaptive Control. New York: Marcel Dekker, Inc..

Mendel, J.M. (2001). Uncertain rule-based fuzzy logic systems: Introduction and new directions. Prentice Hall PTR, Upper Saddle River, NJ.

Mittal, K., Jain, A., Singh Vaisla, K., Castillo, O., and Kacprzyk, J. (2020). A comprehensive review on type 2 fuzzy logic applications: Past, present and future. Engineering Applications of Artificial Intelligence, 95, 103916.

Noshadi, A., Shi, J., Lee, W.S., Shi, P., and Kalam, A. (2016). Optimal PID-type fuzzy logic controller for a multi-input multi-output active magnetic bearing system. Neural Computing and Applications, 27 (7), 2031-2046.

Phan, D., Bab-Hadiashar, A., Fayyazi, M., Hoseinnezhad, R., Jazar, R.N., and Khayyam, H. (2020). Interval type-2 fuzzy logic control for energy management of hybrid electric autonomous vehicles. IEEE Transactions on Intelligent Vehicles, 2020, DOI: 10.1109/TIV.2020. 3011954.

Pozna, C. and Precup, R.-E., An approach to the design of nonlinear state-space control systems. (2018). Stud. Informat. Control, 27 (1), 5-14.

Precup, R.-E., Tomescu, M.-L., and Dragos, C.-A. (2014) Stabilization of Rössler chaotic dynamical system using fuzzy logic control algorithm. Int. J. Gen. Syst., 43 (5), 413-433.

Precup, R.-E., Angelov, P., Costa, B.S.J., and Sayed-Mouchaweh, M. (2015). An overview on fault diagnosis and nature-inspired optimal control of industrial process applications. Computers in Industry, 74, 75-94.

Precup, R.-E. and David. R.-C. (2019). Nature-inspired optimization algorithms for fuzzy controlled servo systems. Butterworth-Heinemann, Elsevier, Oxford.

Precup, R.-E., David, R.-C., and Petriu, E.M. (2017a). Grey wolf optimizer algorithm-based tuning of fuzzy control systems with reduced parametric sensitivity. IEEE Transactions on Industrial Electronics, 64 (1), 527-534.

Precup, R.-E., David, R.-C., Petriu, E.M., Szedlak-Stinean, A.-I., and Bojan-Dragos, C.-A. (2016). Grey wolf optimizer-based approach to the tuning of PI-fuzzy controllers with a reduced process parametric sensitivity. IFAC-PapersOnLine, 49 (5), 55-60.

Precup, R.-E., David, R.-C., Szedlak-Stinean, A.-I., Petriu, E.M., and Dragan, F. (2017b). An easily understandable grey wolf optimizer and its application to fuzzy controller tuning. Algorithms, 10 (2), 68.

Precup, R.-E. and Preitl, S., (1997). Popov-type stability analysis method for fuzzy control systems, in Proc. Fifth Europ. Congr. Intell. Tech. Soft Comp., Aachen, Germany, 2, 1306-1310.

Precup, R.-E. and Preitl, S., (2003). Popov-type stability analysis method for fuzzy control systems with PI fuzzy controllers, Rev. Roum. Sci. Tech. Electr. Ener. Ser., 48 (4), 505-522.

Precup, R.-E., Preitl, S., Petriu, E. M., Roman, R.-C., Bojan-Dragoş, C.-A., Hedrea, E.-L., and Szedlak-Stînean, A.-I. (2020). A center manifold theory-based approach to the stability analysis of state feedback Takagi-Sugeno-Kang fuzzy control systems, Facta Universitatis, Series: Mechanical Engineering (University of Nis), 18 (2), 189-204, impact factor (IF) = 3.324, IF according to 2020 Journal Citation Reports (JCR) released by Clarivate Analytics in 2021 = 3.324 (casopisi.junis.ni.ac.rs).

Precup, R.-E., Preitl, S., Solyom, S., (1999). Center manifold theory approach to the stability analysis of fuzzy control systems, in Computational Intelligence. Theory and Applications, Reusch, B., Ed., Springer-Verlag, Berlin, Heidelberg, New York, Lecture Notes in Computer Science, 1625, 382-390.

Taghavifar, H. and Rakheja, S. (2019). Path-tracking of autonomous vehicles using a novel adaptive robust exponential-like-sliding-mode fuzzy type-2 neural network controller. Mechanical Systems and Signal Processing, 130, 41-55.

D. Results in 2021

Precup, R.-E., Roman, R.-C., Hedrea, E.-L., Petriu, E. M. and Bojan-Dragoş, C.-A. (2021a). Data-Driven Model-Free Sliding Mode and Fuzzy Control with Experimental Validation, International Journal of Computers Communications & Control (Agora University Editing House - CCC Publications), 16 (1), 4076, 1-17, impact factor

(IF) = 2.293, IF according to 2020 Journal Citation Reports (JCR) released by Clarivate Analytics in 2021 = 2.293 (univagora.ro/jour/).

Precup, R.-E., David, R.-C., Roman, R.-C., Petriu, E. M., Szedlak-Stinean, A.-I. (2021b). Slime Mould Algorithm-Based Tuning of Cost-Effective Fuzzy Controllers for Servo Systems, International Journal of Computational Intelligence Systems, 14 (1), 1042–1052, impact factor (IF) = 1.736, IF according to 2020 Journal Citation Reports (JCR) released by Clarivate Analytics in 2021 = 1.736.

Precup, R.-E., Bojan-Dragoş, C.-A., Hedrea, E.-L., Roman, R.-C. and Petriu, E. M. (2021c). Evolving Fuzzy Models of Shape Memory Alloy Wire Actuators, Romanian Journal of Information Science and Technology (Romanian Academy, Section for Information Science and Technology), accepted, to be published in 24 (4), 1-13, impact factor (IF) = 0.643, IF according to 2020 Journal Citation Reports (JCR) released by Clarivate Analytics in 2021 = 0.643.

Bojan-Dragoş, C.-A., Precup, R.-E., Preitl, S., Roman, R.-C., Hedrea, E.-L. and Szedlak-Stînean, A.-I. (2021). GWO-Based Optimal Tuning of Type-1 and Type-2 Fuzzy Controllers for Electromagnetic Actuated Clutch Systems, Proceedings of 4th IFAC Conference on Embedded Systems, Computational Intelligence and Telematics in Control CESCIT 2021, Valenciennes, France, 2021, IFAC-PapersOnLine, 54 (4), 189-194, indexed in Scopus.

Hedrea, E.-L., Precup, R.-E., Roman, R.-C., Petriu, E. M., Bojan-Dragoş, C.-A. and Hedrea, C. (2021). Tensor Product-Based Model Transformation Technique Applied to Servo Systems Modeling, Proceedings of 30th International Symposium on Industrial Electronics ISIE 2021, Kyoto, Japan, 1-6, indexed in IEEE Xplore.

Roman, R.-C., Precup, R.-E., Hedrea, E.-L., Preitl, S., Zamfirache, I. A., Bojan-Dragoş, C.-A. and Petriu, E. M. (2021). Iterative Feedback Tuning Algorithm for Tower Crane Systems, Proceedings of 8th International Conference on Information Technology and Quantitative Management ITQM 2020 & 2021, Chengu, China, 1-8, to be published in Procedia Computer Science (Elsevier).

Director of the Project,

BOJAN-DRAGOȘ Claudia-Adina